# A Non-Contact Thermal Barrier Coating (TBC) Heat Flux Sensor Using a Self Calibrating Multiwavelength Pyrometer

Daniel Ng and Charles M. Spuckler
*Lewis Research Center*
*Cleveland, Ohio*

January 1996

# A NON-CONTACT THERMAL BARRIER COATING (TBC) HEAT FLUX SENSOR USING A SELF CALIBRATING MULTIWAVELENGTH PYROMETER

DANIEL NG
NASA Lewis Research Center
Cleveland, OH 44135

CHARLES M. SPUCKLER
NASA Lewis Research Center
Cleveland, OH 44135

## Abstract

Non-contact heat flux measurements have been demonstrated using crystalline sapphire and polycrystalline alumina as the working material and a multiwavelength pyrometer as the measuring device. Heat flux sensing is now achieved using a 25 μm thick nanostructured thermal barrier coating (TBC) on 3 mm thick sapphire substrate. Advanced nanostructured TBCs transmits in the infrared region and are capable of producing even larger temperature differences than the traditional flame sprayed zirconia TBC. Though a 1 mm (40 mil) thick flame sprayed zirconia TBC produced the desired temperature difference, it transmitted less than 0.2 % of the radiation in the short wavelength region, making it less suitable as a heat flux sensor.

## Introduction

A non-contact heat flux gauge using semi-transparent material was demonstrated using a sapphire crystal[1] and polycrystalline alumina[2] as the working material and a multiwavelength pyrometer as the measuring device. The successes obtained so far indicated that it may be possible to make a heat flux sensor from the protective thermal barrier coating (TBC) materials that are widely used on turbine engine components. The traditional flame sprayed zirconia ($ZrO_2$) TBC and a new nanostructured TBC were investigated.

## Method

The design of a remote heat flux sensor was described in refs. 1 & 2. Figures 1 and 2 illustrate the concept and its implementation. The sensor consists of a semi-transparent material slab of thickness t, thermal conductivity κ, and cross-sectional area A. The temperature difference $\Delta T = T_2 - T_1$ across the surface of this heat flux sensor is measured using a multiwavelength pyrometer exploiting the fact that short wavelength radiation originates in the back and long wavelength radiation originates at the front of the semitransparent material. The conducted heat flux is determined from Eqn. 1 where Q is the rate of thermal energy conducted across the area A arising from the temperature gradient $\Delta T/t$.

$$\dot{Q}/A = \kappa (\Delta T/t) \tag{1}$$

The ability to measure the front and back surface temperatures of the sensor depends on knowing the emissivity and transmissivity of the material involved. These quantities are shown in figures 3 & 4 for crystalline sapphire and polycrystalline alumina. Above 6 μm, there is essentially no transmission for the 8 mm thick sapphire. Alumina, being chemically the same as sapphire, is expected to have similar transmissivity and emissivity at long wavelengths (>7 μm). The alumina transmissivity shown in figure 4 is different from that of sapphire in figure 3. Alumina transmits much less than the sapphire and the transmission exhibits a maximum attributed to losses due to scattering by the polycrystals constituting the material. This is consistent with the data in ref. 3 which shows that in

this wavelength range the scattering decreases with wavelength. The emissivity of sapphire[2] and alumina are very similar.

Flame sprayed zirconia ($ZrO_2$) is the prime TBCs candidate for a heat flux sensor because it is widely used on turbo machinery components[5]. $ZrO_2$ emissivity is very low, at short ($\lambda < 4$ μm) wavelengths. It increases to unity at the longer ($\lambda > 8$ μm) wavelengths[5] with the transmissivity being zero there. Free standing $ZrO_2$ TBCs of thickness 0.125, 0.25, 0.5 and 1 mm were prepared. By positioning them between a 1335 K black body radiation source and a chopper, their transmissions at room temperature were measured (figure 5). The energy is attenuated by absorption, scattering and interface reflections. The thickness of TBC on turbo machinery components are of the order 0.1 mm. A 0.125 mm thick sample of $ZrO_2$ transmitted less than 2% of the radiation. The transmitted energy may not be enough to perform temperature measurements. Also, the 0.125 mm thick material would not produce a large enough temperature difference to be measurable by the pyrometer. Low transmission and small temperature differences may rule out traditional flame sprayed $ZrO_2$ TBC as a heat flux sensor.

A new nanostructure is being developed for use as a TBC on engine components. These TBCs are more effective thermal insulators. The composition and structure of these coatings are proprietary. TBCs, only 25 μm (0.025 mm) thick, produced large temperature differences. The transmission of a nanostructured TBC on zinc selenide is shown in figure 6. Radiation is from the visible up to 10 μm. Zinc selenide, transmits up to 14 μm, indicating that the nanostructured TBC layer is transparent up to about 10 μm. The apparent low transmission in figure 6 is due to the 6 mm polycrystalline zinc selenide substrate which strongly scatters and therefore attenuates radiation. A nanostructure coating was obtained on a 3 mm thick sapphire disk. Heat flux sensing was accomplished using this nanostructure sample.

Results

The transmission spectra (figure 7) of nanostructured material on sapphire at short wavelengths ($\lambda < 6$ μm) was obtained by placing the sample in front of a black body furnace set to different temperatures. Because the black body temperatures are known (1339, 1215, 1092, 974, 862 and 751 K), the transmissivity (figure 8) of the nanostructured TBC sapphire combination was obtained by dividing the spectra by the Planck functions at these temperatures. The absorption, scattering and interface reflections are accounted for using this technique. Though the nanostructured TBC itself transmits up to 10 μm, the nanostructured TBC sapphire combination does not transmit above 6 μm due to the sapphire. The emission spectra of the nanostructure sapphire combination at long ($\lambda > 6$ μm) wavelength is shown in figure 9. The emissivity in this spectral region is taken to be unity. Planck curves of different temperatures and emissivity of unity fit the emission spectra very well in the 10 to 13 μm region. In this way, the temperature of the nanostructure surface viewing the spectrometer were determined to be 575, 540, 495, 462 and 421 K. The nanostructured TBC is made into a heat flux sensor in the same manner as sapphire and alumina[1-2]. The surface of the sapphire that did not have the nanostructured TBC on it was coated with scanning electron microscopy black graphite paint and placed in the opening of a black body furnace which was set to various temperatures. The painted surface looked into the furnace. The emissivity of this graphite paint, measured previously[1], is shown in figure 10. Radiant energy from the black body furnace reaching the painted sapphire surface is dissipated by the following mechanisms: (i) reflected and emitted by the graphite surface back into the furnace, (ii) conducted through the graphite paint, the sapphire, and the nanostructured TBC and then convected and radiated away from the front surface, (iii) radiated from the graphite surface and transmitted through the sapphire and nanostructured TBC exiting from its front surface.

Spectra of nanostructured TBC sapphire with a graphite paint on one surface were obtained at different black body furnace temperatures. They are shown in figure 11. Each of these spectra is assumed to consist of two parts, (i) radiation emitted by the graphite paint and transmitted through

the sapphire and nanostructured TBC, and (ii) radiation emitted from the front surface of the nanostructured TBC. The spectra are represented by:

$$S(\lambda) = \varepsilon_1(\lambda) \tau(\lambda) L_\lambda(T_1) + \varepsilon_2(\lambda) L_\lambda(T_2) \qquad (2)$$

where $\varepsilon_1$ is the graphite emissivity, $\tau$ is the sapphire and nanostructured TBC transmissivity and $\varepsilon_2$ is the nanostructured TBC emissivity.

The two components in Eqn. 2 were calculated:

(i)    **The Back Surface (graphite)** component was calculated from a Planck function corresponding to the graphite temperature, the averaged short wavelength transmissivity (which included all interface reflections) of nanostructured TBC coated sapphire (figure 8), and the graphite paint emissivity (figure 10).

(ii)   **The Front Surface (nanostructured TBC)** component was calculated from a Planck function corresponding to the front surface temperature of the nanostructure TBC and the unity emissivity in this range which was used to fit the data in figure 9 at wavelengths $\lambda > 10$ µm.

The data in fig. 12 is the sum of these two components. The dip between 4 and 6 µm is due to the complex absorption and re-emission process which is neglected at the present time. The other curves are the measured spectrum, and two Planck functions (one for the front surface and one for the graphite paint). The graphite temperature was determined to be 752.4 K and the nanostructure front surface temperature to be 687 K. The same analysis was performed on the other spectra in figure 11. The graphite temperatures were determined to be 752.4, 658.0, 571.9, 508.0, 460.8 and 427.4 K and temperature differences, $\Delta T$, across the nanostructured TBC and sapphire were 65.4, 48.0, 31.9, 28.0, 27.8 and 27.4 K respectively. On interface reflection has to be eliminated to obtain the correct temperature.

Similar to the sapphire and alumina heat flux sensors, the determination of the graphite temperature depended critically on knowing the sensor material transmissivity. The nanostructured TBC-sapphire transmissivity shown in figure 8 was measured previously from the transmission spectra, which includes all interface reflections. While with the graphite paint on a surface to make a heat flux sensor, one interface reflection is eliminated. The graphite emissivity shown in figure 10 was measured in air. Once the nanostructured TBC is deposited on a surface, it is not possible to measure the emissivity of the substrate and the transmissivity of the TBC independently. The recently developed self-calibrating, emissivity and/or transmissivity independent multiwavelength pyrometer[6] was adapted to measure in situ the surface emissivities, the TBC transmissivity and the back surface temperature of the heat flux sensor all at once. This corrects for the interface reflection.

The measured spectrum $S(\lambda,T)$ of a surface in volts is related to the radiation constants $c_1$, $c_2$, and the temperature $T$ in Planck's law, the emissivity $\varepsilon_\lambda$ of the graphite paint-sapphire interface, the transmissivity $\tau_\lambda$ of the sapphire and nanostructured TBC, and the instrument constant $g_\lambda$ (representing the radiation to voltage conversion constant of the detector in the pyrometer) by

$$S(\lambda, T(t_j)) = g_\lambda \tau_\lambda \varepsilon_\lambda \frac{c_1}{\lambda^5} \frac{1}{\exp(c_2/\lambda T(t_j)) - 1} \qquad (3)$$

Because the spectra in figure 11 were recorded at different times, we designate them as $S(\lambda,(t_j))$, where $T(t_j)$ is the temperature at time $t_j$. Consider 2 wavelengths, labeled $\lambda_R$ and $\lambda_T$ at time $t$ and their associated quantities. Eqn. 3 is used for each wavelength. The two resulting equations are solved for $T(t)$ and set equal to each other yielding

$$T(t) = \frac{c_2/\lambda_R}{\log_e\left(g_R\varepsilon_R\tau_R\dfrac{c_1}{\lambda_R^5}\dfrac{1}{S(\lambda_R,t)}+1\right)} = \frac{c_2/\lambda_I}{\log_e\left(g_I\varepsilon_I\tau_I\dfrac{c_1}{\lambda_I^5}\dfrac{1}{S(\lambda_I,t)}+1\right)} \qquad (4)$$

.

Solving this equation for $S(\lambda_I,t)$ gives

$$S(\lambda_I,t) = g_I\varepsilon_I\tau_I\left\{\frac{\dfrac{c_1}{\lambda_I^5}}{\left(g_R\varepsilon_R\tau_R\dfrac{c_1}{\lambda_R^5}\dfrac{1}{S(\lambda_R,t)}+1\right)^{\frac{\lambda_R}{\lambda_I}}-1}\right\} \qquad (5)$$

Any additional constants, such as refractive index dependence at each wavelength can be lumped together inside $g_\lambda$. Referring to Eqn. 5, by assigning a value to $g_R\varepsilon_R\tau_R$, the quantity in the curly bracket on the right hand side is evaluated from the spectra data and is plotted vs the quantity on the left hand. The resulting straight line passes through the origin with a slope equal to $g_I\varepsilon_I\tau_I$. The slope is determined by least squares method. Using a set of data represented by the spectra $S(\lambda,t)$, $g_I\varepsilon_I\tau_I$ is defined in terms of $g_R\varepsilon_R\tau_R$. This is done for all I≠R. The $g_I\varepsilon_I\tau_I$s are now functions of $g_R\varepsilon_R\tau_R$ only. Temperatures $T(\lambda,t)$ can now be determined from Eqn. 6 (derived from Eqn. 4).

$$T(\lambda,t) = \frac{c_2/\lambda_I}{\log_e\left(g_I\varepsilon_I\tau_I\dfrac{c_1}{\lambda_I^5}\dfrac{1}{S(\lambda_I,t)}+1\right)} \qquad (6)$$

In theory, at time t, $T(\lambda,t)$ has no wavelength dependence and should be equal to each other. For real data, there will be variations, and averages of $T(t)$ over all wavelengths are defined as

$$T(t) = \frac{\sum_{I=1}^{I=N} T(\lambda_I,t)}{N} \qquad (7)$$

Among the many possible values of $g_R\varepsilon_R\tau_R$, the correct one is selected by using the following least squares procedure:

1) Assign a value to $g_R\varepsilon_R\tau_R$, determine the corresponding $g_I\varepsilon_I\tau_I$ using Eqn. 5.
2) Use the so determined $g_I\varepsilon_I\tau_I$ to determine $T(t)$ using Eqns. 6&7.
3) Transform all the spectra into a large data set (x,y) using

$$x = c_2/\lambda T(t) \quad , \quad y = \frac{S(\lambda,t)}{g_\lambda\varepsilon_\lambda\tau_\lambda}\frac{1}{T(t)^5} = \frac{c_1}{c_2^5}\frac{x^5}{e^x-1} \qquad (8)$$

4) The transformed data set (x,y) obeys the generalized non-dimensional Planck formula (Eqn. 8, an invariant curve). The (x,y) data is fitted to the Planck curve by evaluating the residuals. The residual is the sum of the squares of the transformed y minus the calculated y, which is obtained using the transformed x data in the y formula defined in Eqn 8.
5) A new value is assigned to $g_R\varepsilon_R\tau_R$, and steps (1 to 4) repeated.
The value of $g_R\varepsilon_R\tau_R$ that produced the least residual is the correct one, and determines the corresponding $g_I\varepsilon_I\tau_I$ and $T(t)$.

To perform the data analysis, it was more convenient to transformed the data by selecting one of the

4

spectra as a reference and subtracting it from all the other spectra and work with the differences. Because no signal of wavelength longer than 6 μm is transmitted through the TBC sapphire combination, only this portion of the spectra in figure 11 was used to determine the back surface temperature. Figure 13 shows a plot of data using to Eqn. 5. It is indeed a straight line. The slope is obtained by least squares curve fitting. The resulting $g_f\varepsilon_f\tau_t$s are shown in figure 14, which contains the product of the nanostructured TBC sapphire transmissivity and the graphite emissivity, and the front surface emissivity. Beyond 4.5 μm, the combined effect of surface emission and absorption and emission in the transparent material is evident. Also shown in figure 14 is the average nanostructured TBC sapphire transmissivity from fig. 8. Figure 15 shows the calculated temperatures $T(\lambda,t)$. The results from high temperature spectra whose data have good signal to noise ratio, exhibited almost constant temperatures. As the temperature drops, the peak energy moves to longer wavelengths. Therefore the spectra for low temperatures have poor signal to noise ratio, especially at shorter wavelengths, with some of the data being negative. Eqn. 6 cannot process a negative argument in the logarithm function, thus producing no valid temperatures. The transformed (x,y) data are shown in figure 16 together with the invariant non-dimensional Planck curve. The data corresponding to the 3 lowest temperature spectra showed considerable scatter because of the poor signal to noise inherent at low temperatures and short wavelengths. The "poor" data that could not be processed by Eqn. 6 were excluded from evaluating T(t) using Eqn. 7, but are included in curve fitting using Eqn. 8. If they were excluded, most of the scatter in the data in figure 16 would definitely be removed. But the agreement is unmistakable. The temperatures of the graphite paint sapphire interface were determined to be 744.6, 651.2, 567.5, 494.2, 443.6 and 409.1 K. These temperatures agree to within about 5% with temperatures obtained using prior determined nanostructured TBC-sapphire transmissivity and graphite surface emissivity obtained from experimental conditions not exactly identical to the situation when the heat flux was measured. The nanostructured TBC front surface temperatures, calculated using data at the 11 to 12 μm wavelength region, are 694.0, 612.1, 539.3, 481.8, 433.5 and 401.0 K. The resulting temperature differences are 50.6, 39.1, 28.2, 12.4, 10.1 and 8.1 K.

The thermal energy absorbed by the graphite paint is taken to be $\varepsilon_{avg}\sigma(T_{BB}^4 - T_\varepsilon^4)$, where $\sigma = 5.67032 \times 10^{-8}$ W/m$^2$K$^4$ is the Stefan-Boltzmann's constant, $T_{BB}$ is the black body furnace temperature, $T_\varepsilon$ is the graphite paint temperature, and $\varepsilon_{avg}$ is the average emissivity of graphite paint taken to be 0.8. The calculated heat fluxes are 133.6, 91.5, 60.2, 38.2, 23.3 and 13.1 kW/m$^2$. The plot of the incident heat flux vs temperature difference obtained using the two procedures are shown in figure 17. To obtain heat flux values from the pyrometer measured temperature difference requires knowing the nanostructured TBC thermal conductivity and thickness. If $t_s$ is the sapphire thickness and $t_n$ is the nanostructure TBC thickness, then $t = t_\varepsilon + t_s$ is the total nanostructured TBC and sapphire thickness. If $\kappa_s$ is the thermal conductivity of sapphire and $\kappa_n$ is the thermal conductivity of nanostructured TBC; then the equivalent thermal conductivity $\kappa_e$ of them combined is given by

$$\frac{t}{\kappa_e} = \frac{t_s + t_n}{\kappa_e} = \frac{t_s}{\kappa_s} + \frac{t_n}{\kappa_n} \tag{9}$$

Precise values of $t_n$ and $\kappa_n$ are not available, $t_n$ is known only to be about 25 μm. The slopes of the two lines in figure 17 is the quantity $\kappa_e/t$. They are evaluated to be 1.89 and 2.43 kWm$^{-2}$K$^{-1}$ respectively. For $t_n = 25$ μm, $t_s = 3.4$ mm, and $\kappa_s$ being between about 15 to 30 Wm$^{-1}$K$^{-1}$, and the value 2.43 selected for $\kappa_e/t$, $\kappa_n$ is determined to be between 0.0064 and 0.0062 Wm$^{-1}$K$^{-1}$. This is about five thousand times less than sapphire or alumina. The new nanostructured TBCs would make a very good heat flux sensor.
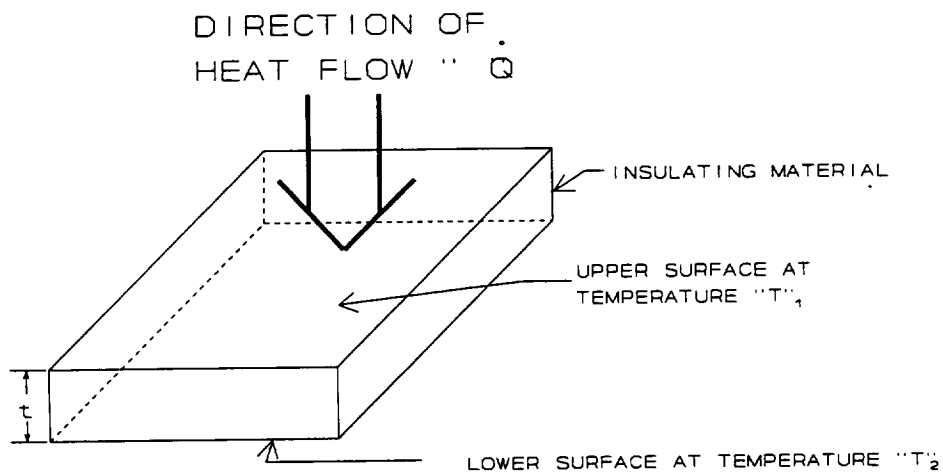
Conclusion

The traditional zirconia TBC coating of usual thickness (0.1 mm) may not transmit enough optical

signal to function as a heat flux sensor. A 25 μm nanostructured TBC on a 3 mm thick sapphire substrate developed sufficient temperature difference between its two surfaces to be measured by a multiwavelength pyrometer and used for heat flux measurements. Based on the estimated thermal conductivity, a 25 μm thick nanostructure TBC should produce a sufficient temperature gradient to be used as a heat flux gauge.
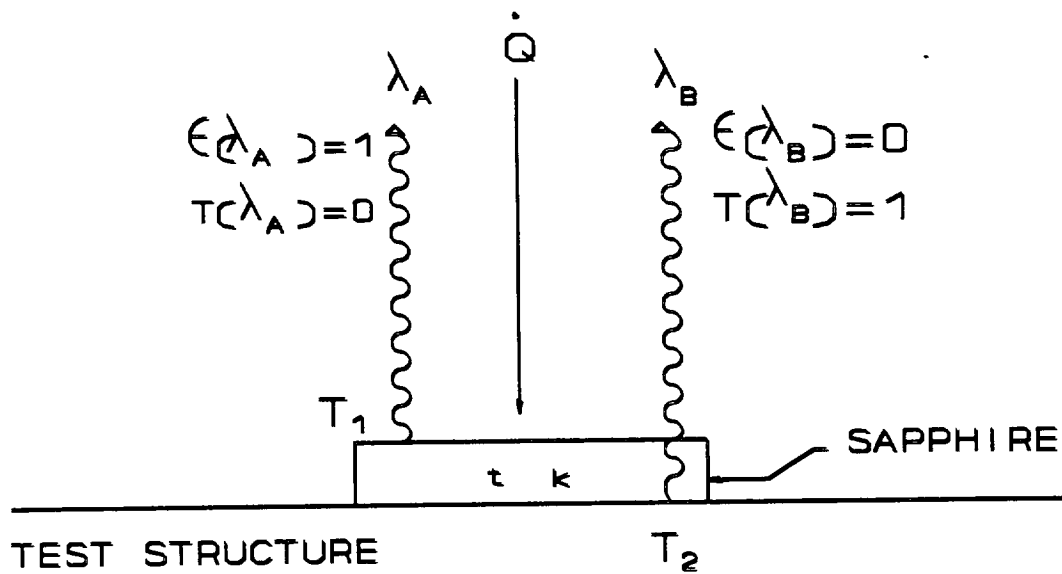
## References

1    Ng, Daniel, Spuckler, Charles M., "Non-contact Heat Flux Measurement Using a Transparent Sensor", NASA TM 106252, July 1993.

2    Ng, Daniel, Spuckler, Charles M., "Non-contact Alumina Heat Flux Sensor", NASA Conference Publication 10146, HITEMP Review 1994, page 26-1 to 26-12.

3    Makino, T., Kunitomo, T., Sakai, I., and Kinoshita, H., "Thermal Radiation Properties of Ceramic Materials," Heat Transfer - Japanese Research, Vol. 13, Oct.-Dec. 1984, pp. 33-50.

4    Sova, R. M., Linevsky, M. J., Thomas, M. E., Mark, F. F., "High Temperature Optical Properties of Oxide Dome Materials", SPIE Proceeding, Vol. 1760, 1992.

5    Liebert, C., "Emittance and absorptance of NASA Ceramic Thermal Barrier Coating System", NASA Technical Paper 1190, 1978, Lewis Research Center, Ohio.

6    Ng, Daniel, Temperature Measurement of $ZrO_2$ TBC Using a Simplified Self Calibrating Multiwavelength Pyrometer, NASA Conference Publication 10178, HITEMP Review 1995, Paper 40.

7    American Institute of Physics Handbook, 3rd Edition, 1972, McGraw Hill, New York, NY, page 4-159.

DIRECTION OF
HEAT FLOW " $\dot{Q}$

INSULATING MATERIAL

UPPER SURFACE AT
TEMPERATURE "T"$_1$

$t$

LOWER SURFACE AT TEMPERATURE "T"$_2$

$$\dot{Q} = \frac{K(T_1 - T_2)}{t}$$

Schematic of a heat flux sensor.

**Figure 1**

$\lambda_A$ $\dot{Q}$ $\lambda_B$

$\epsilon(\lambda_A)=1$ $\epsilon(\lambda_B)=0$

$T(\lambda_A)=0$ $T(\lambda_B)=1$

$T_1$ SAPPHIRE

$t$ $k$

TEST STRUCTURE $T_2$

Two Optical Region Heat Flux Sensor.

**Figure 2**

7

TRANSMISSIVITY–room temp
EMISSIVITY    – 950 K
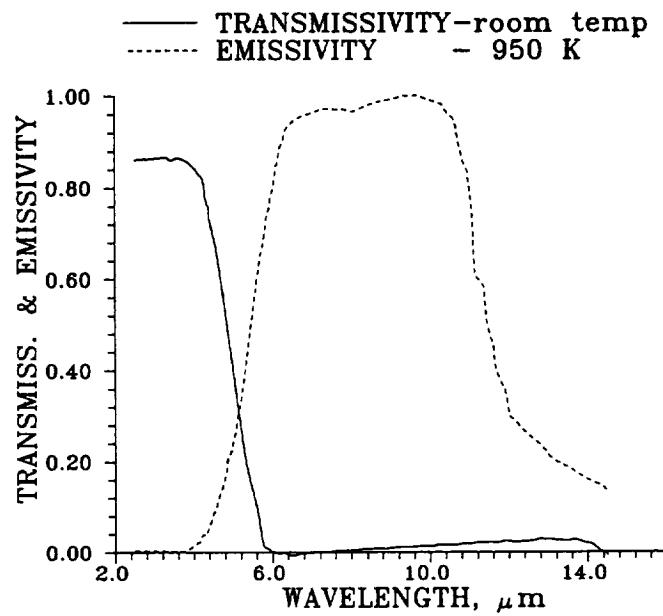
The Emissivity of Sapphire (ref. 4) and Transmissivity of 8 mm Thick Sapphire (ref. 1)

**Figure 3**



TRANSMISSIVITY
EMISSIVITY
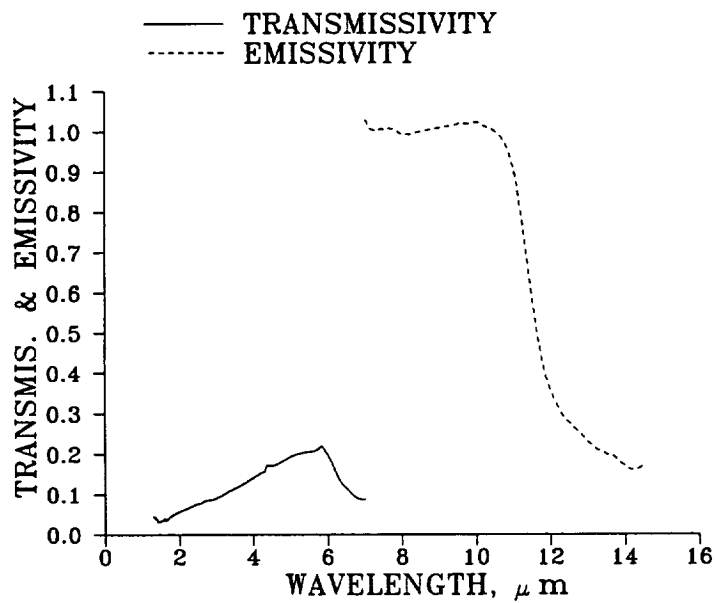
The emissivity and transmissivity of 1.26 mm thick alumina.

**Figure 4**

8
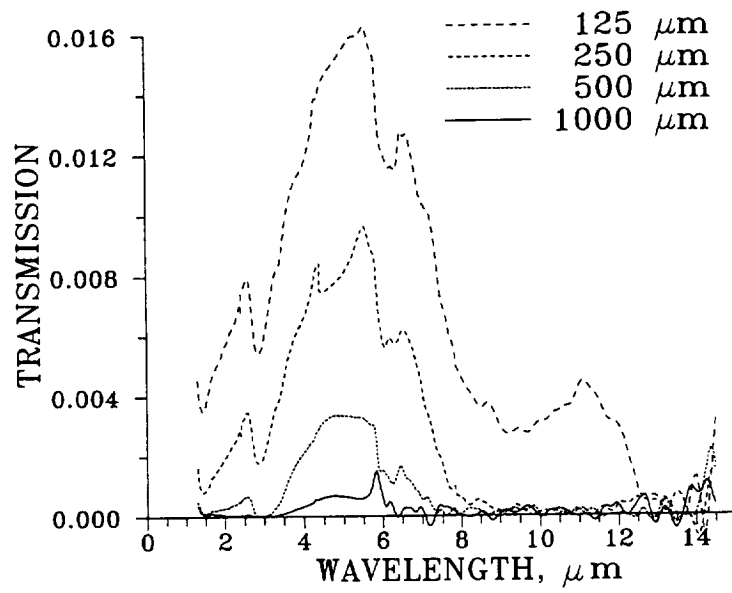
**Figure 5**
Transmission of zirconia TBCs of different thickness.
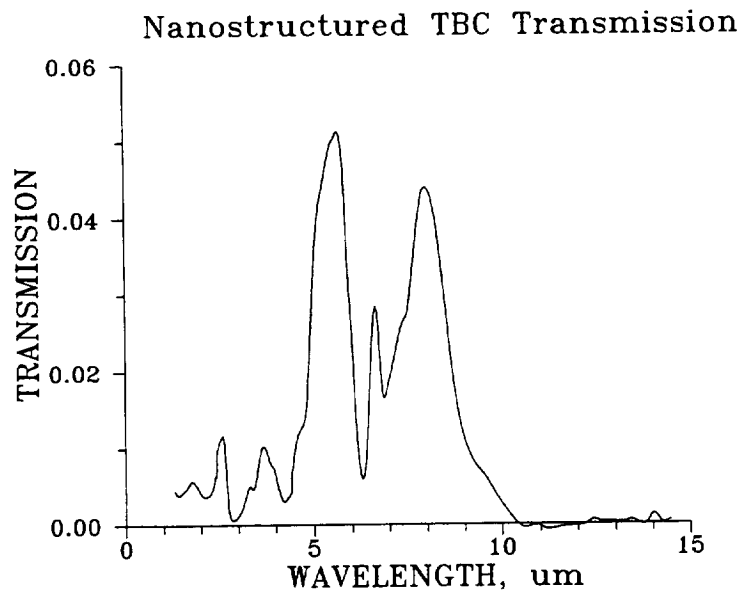


Transmission of nanostructured TBC on zinc selenide.

**Figure 6**
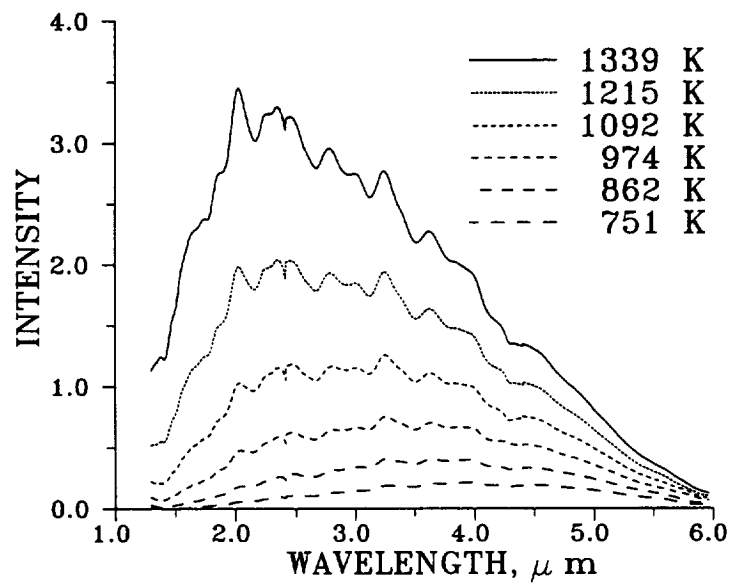
Transmission spectra of nanostructured TBC on sapphire.

**Figure 7**
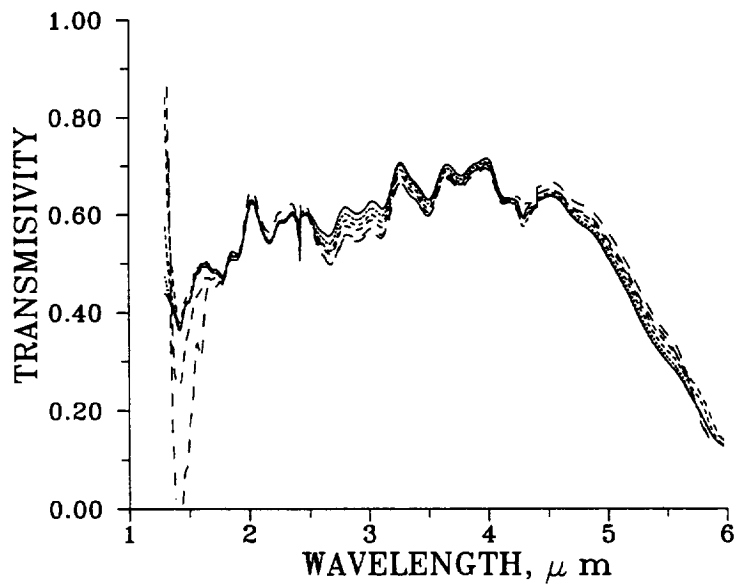


Transmission of nanostructured TBC sapphire combination.

**Figure 8**
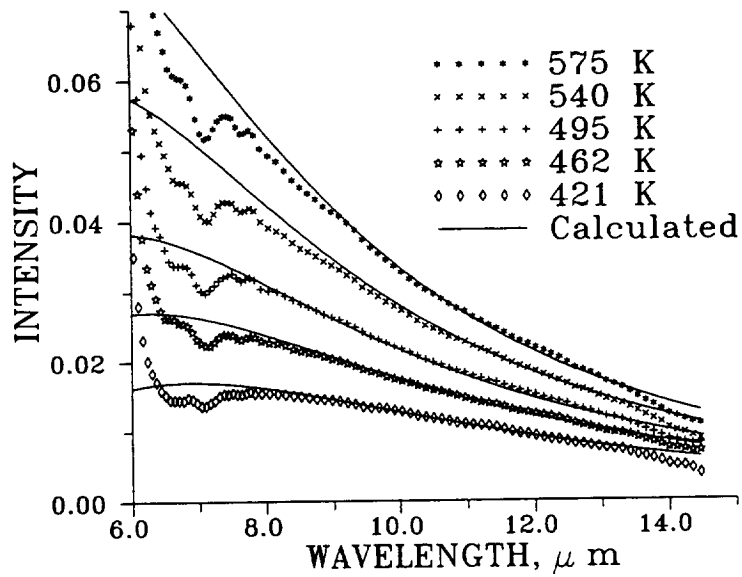
Emission spectra of nanostructured TBC on sapphire.

**Figure 9**
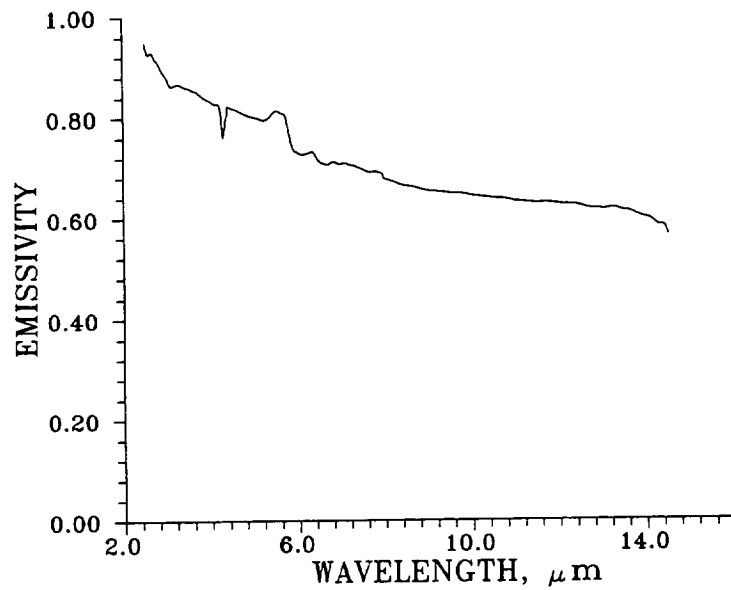


Emissivity of graphite paint (ref. 1).

**Figure 10**
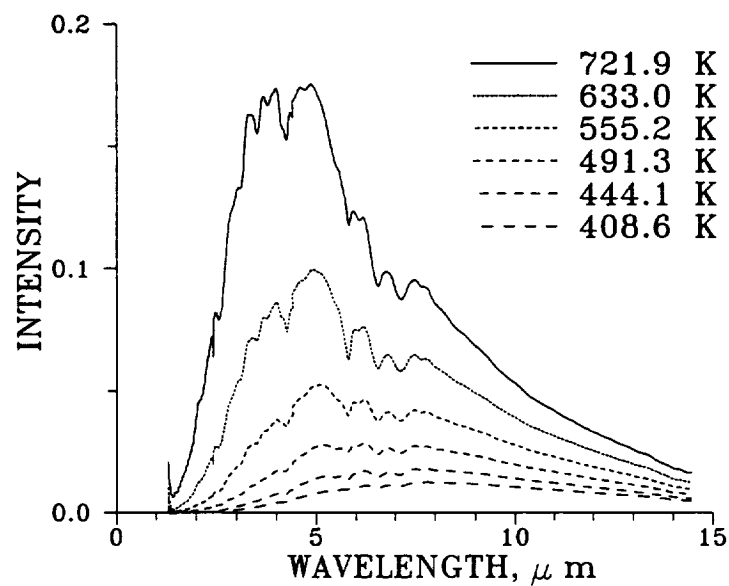
Spectra of nanostructured TBC on sapphire with graphite paint on one surface for different black body furnace temperatures.

**Figure 11**
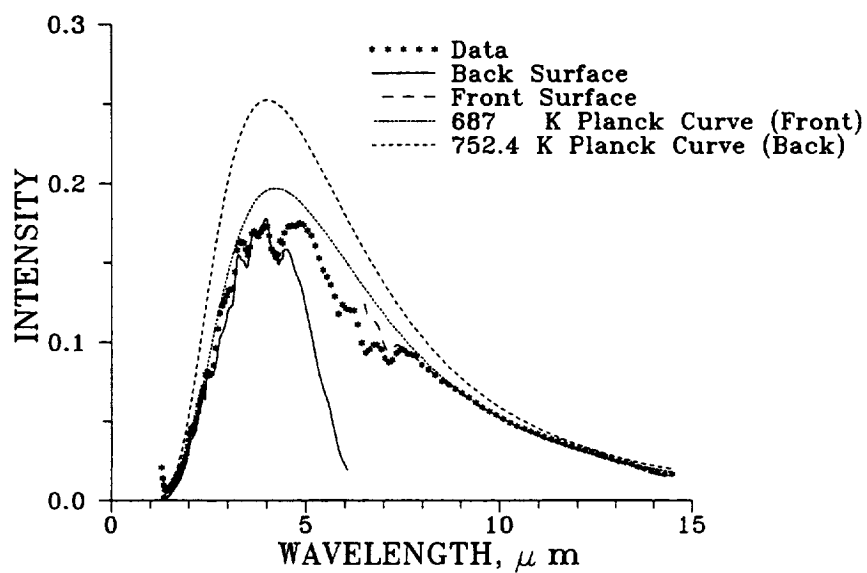


Fitted spectrum of nanostructured TBC on sapphire with graphite paint on back surface.

**Figure 12**
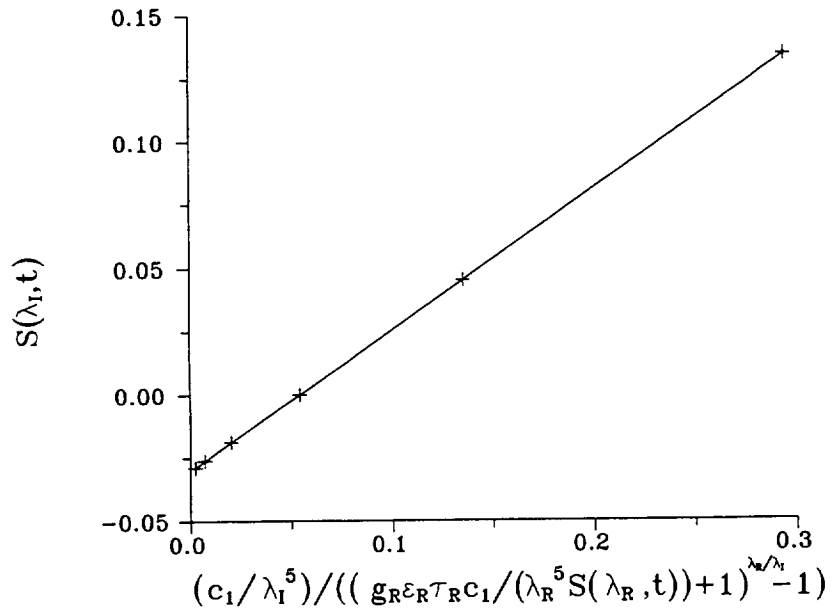
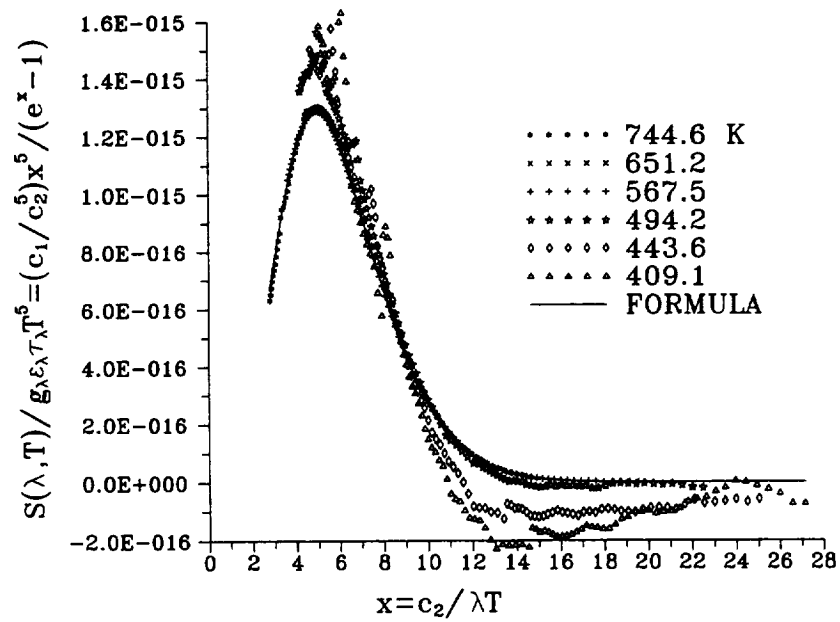Plot of data according to Equation 5, $\lambda_R$=4.736 μm, $\lambda_I$=3.6 μm.

**Figure 13**



——— $g_I \varepsilon_I \tau_I$ using self calibration method
- - - - Transmission Determined in Figure 8
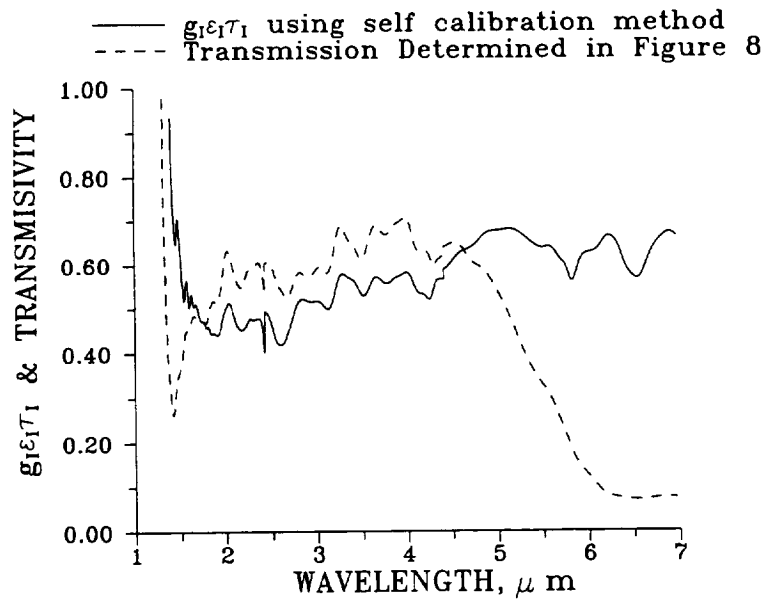
$g_i \varepsilon_i \tau_i$ from self calibration method and transmission of nanostructured TBC on sapphire measured separately.
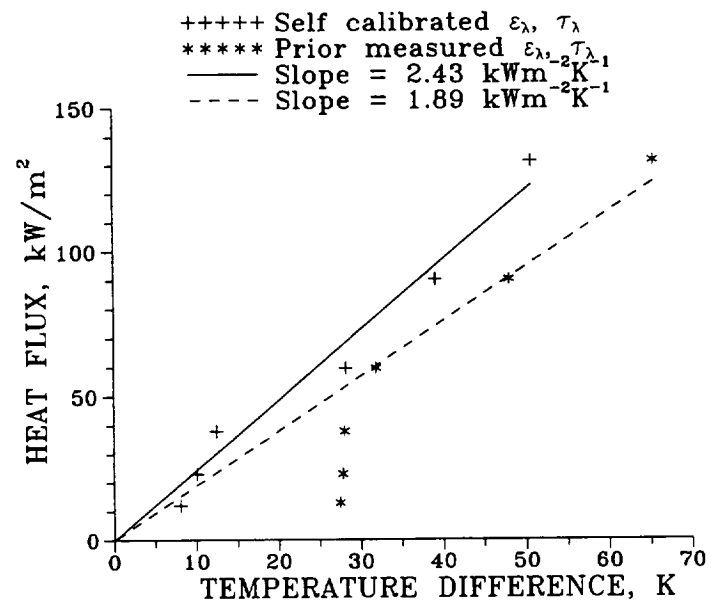
**Figure 14**

13
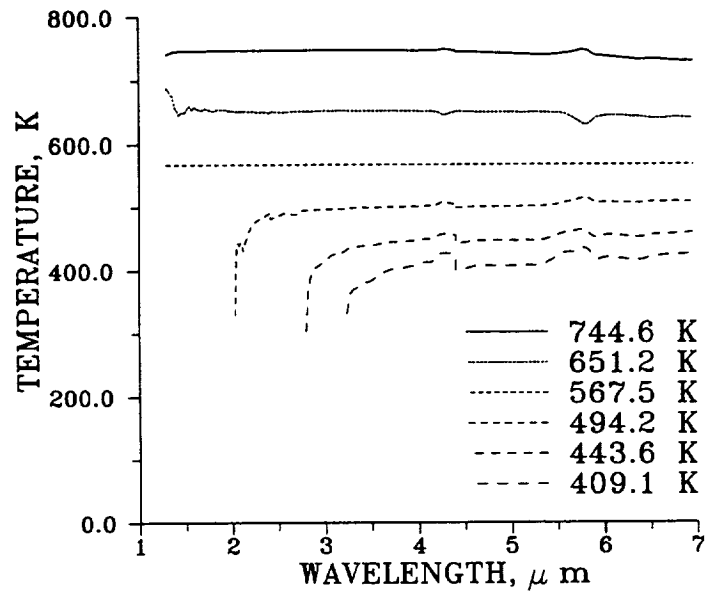
Temperatures calculated from spectra using $g_i \varepsilon_i \tau_i$ and Equation 6.
**Figure 15**



Data transformed according to Eqn. 8 fitted to the generalized non-dimensional Planck equation.

**Figure 16**

14

Incident Heat Flux vs. Temperature difference across the nanostructure TBC on sapphire.

**Figure 17**

# REPORT DOCUMENTATION PAGE

| 1. AGENCY USE ONLY (Leave blank) | 2. REPORT DATE | 3. REPORT TYPE AND DATES COVERED |
|---|---|---|
| | January 1996 | Technical Memorandum |

**4. TITLE AND SUBTITLE**

A Non-Contact Thermal Barrier Coating (TBC) Heat Flux Sensor Using a Self Calibrating Multiwavelength Pyrometer

**5. FUNDING NUMBERS**

WU–505–90–51

**6. AUTHOR(S)**

Daniel Ng and Charles M. Spuckler

**7. PERFORMING ORGANIZATION NAME(S) AND ADDRESS(ES)**

National Aeronautics and Space Administration
Lewis Research Center
Cleveland, Ohio 44135–3191

**8. PERFORMING ORGANIZATION REPORT NUMBER**

E–10088

**9. SPONSORING/MONITORING AGENCY NAME(S) AND ADDRESS(ES)**

National Aeronautics and Space Administration
Washington, D.C. 20546–0001

**10. SPONSORING/MONITORING AGENCY REPORT NUMBER**

NASA TM–107150

**11. SUPPLEMENTARY NOTES**

Responsible person, Daniel Ng, organization code 2510, (216) 433–3638.

**12a. DISTRIBUTION/AVAILABILITY STATEMENT**

Unclassified - Unlimited
Subject Category 35

This publication is available from the NASA Center for Aerospace Information, (301) 621–0390.

**12b. DISTRIBUTION CODE**

**13. ABSTRACT (Maximum 200 words)**

Non-contact heat flux measurements have been demonstrated using crystalline sapphire and polycrystalline alumina as the working material and a multiwavelength pyrometer as the measuring device. Heat flux sensing is now achieved using a 25 µm thick nanostructured thermal barrier coating (TBC) on 3 mm thick sapphire substrate. Advanced nanostructured TBCs transmits in the infrared region and are capable of producing even larger temperature differences than the traditional flame sprayed zirconia TBC. Though a 1 mm (40 mil) thick flame sprayed zirconia TBC produced the desired temperature difference, it transmitted less than 0.2% of the radiation in the short wavelength region, making it less suitable as a heat flux sensor.

**14. SUBJECT TERMS**

Heat flux; Nanostructure; Pyrometry; Emissivity

**15. NUMBER OF PAGES**

17

**16. PRICE CODE**

A03

| 17. SECURITY CLASSIFICATION OF REPORT | 18. SECURITY CLASSIFICATION OF THIS PAGE | 19. SECURITY CLASSIFICATION OF ABSTRACT | 20. LIMITATION OF ABSTRACT |
|---|---|---|---|
| Unclassified | Unclassified | Unclassified | |

National Aeronautics and
Space Administration

**Lewis Research Center**
21000 Brookpark Rd.
Cleveland, OH 44135-3191